Pure Appl. Chem., Vol. 77, No. 11, pp. 1823–1833, 2005.
DOI: 10.1351/pac200577111823

Is the single transition-state model appropriate for the fundamental reactions of organic chemistry?*

Vernon D. Parker

Department of Chemistry and Biochemistry, Utah State University, Logan, UT 84322-0300, USA

Abstract: In recent years, we have reported that a number of organic reactions generally believed to follow simple second-order kinetics actually follow a more complex mechanism. This mechanism, the reversible consecutive second-order mechanism, involves the reversible formation of a kinetically significant reactant complex intermediate followed by irreversible product formation. The mechanism is illustrated for the general reaction between reactant and excess reagent under pseudo-first-order conditions in eq. i where k_f' is the pseudo-first-order rate constant equal to k_f[Excess Reagent].

Reactant + Excess reagent = Reactant complex + Products (i)

The mechanisms are determined for the various systems, and the kinetics of the complex mechanisms are resolved by our "non-steady-state kinetic data analysis". The basis for the non-steady-state kinetic method will be presented along with examples. The problems encountered in attempting to identify intermediates formed in low concentration will be discussed.

Keywords: Non-steady-state kinetics; mechanism analysis; extent of reaction dependence of KIE; mechanism probes; dynamic residual absorbance analysis.

INTRODUCTION

A prominent goal of physical organic chemists in the 20th century was to develop theoretical relationships that shed light on the structures of the transition states of organic reactions.

Much of the current theory of physical organic chemistry is embodied in the relationships, often based on observed structural effects on reactivity, shown in Fig. 1. These are used to describe the results of the study of the kinetics and mechanisms of organic reactions. What all of these relationships have in common is that they are all most appropriate for the description of reactions that take place in a single step. For reactions involving more than a single transition state, parameters derived from these relationships necessarily become less reliable in describing transition-state structure.

*Paper based on a presentation at the 17th International Conference on Physical Organic Chemistry (ICPOC-17), Shanghai, China, 15–20 August 2004. Other presentations are published in this issue, pp. 1807–1921.

Hammett equation
Brønsted relationship
Hammond postulate
Variable transition-state theory
Marcus relationship
Configuration mixing model
Principle of nonperfect synchronization

Fig. 1 Physical organic chemistry relationships.

Since the work of Eigen [11], it is an accepted fact that all bimolecular reactions in solution pass through an encounter complex (Scheme 1). Because the encounter complex is formed at diffusion-controlled rates, it is not considered to be kinetically significant for reactions taking place on the millisecond or second time scale. Thus, the simple irreversible second-order (simple) and the reversible consecutive second-order (complex) mechanisms are described in Scheme 2 without involving the encounter complexes which are assumed, but not included, in the rate laws. These two mechanisms are kinetically indistinguishable once steady state for the complex mechanism is achieved.

Reactants ⇌ Encounter Complex → Products

$$A + B \underset{k_{-enc}}{\overset{k_{enc}}{\rightleftharpoons}} E.C. \xrightarrow{k_p} C$$

Scheme 1

$$A + B \xrightarrow{k_{simple}} Products \quad \underline{Simple}$$

$$A + B \underset{k_b}{\overset{k_f}{\rightleftharpoons}} I \xrightarrow{k_p} Products \quad \underline{Complex}$$

Scheme 2

In his classic book on physical organic chemistry, Hammett recognized the difficulties in obtaining direct kinetic evidence for the presence of a multi-step reaction mechanism [12]. However, he concluded that "it would require experimental data of more than ordinary precision to recognize effects of this magnitude with any assurance". To my knowledge, there were no serious attempts during the last half of the 20th century to subject the fundamental reactions of organic chemistry, which are assumed to take place by a simple second-order mechanism, to a rigorous mechanism analysis designed to detect a more complex mechanism. During that period, enormous progress was made in digital technology, which provided the tools necessary to undertake this task.

We first realized that it is possible to kinetically distinguish between the simple and complex mechanisms shown in Scheme 2 during our studies of the proton-transfer reactions of methylanthracene radical cations with nitrogen-centered bases [1]. This is made possible by the observation that the reactions taking place by the complex mechanism do not quickly reach a steady state and in the *pre-steady-state* time period, the kinetic response deviates significantly from that expected for the simple single-step mechanism. The work presented here is a summary of the state of the art of non-steady-state kinetics to characterize and resolve the kinetics of a number of fundamental organic reactions that are best described by the two consecutive transition-state models [1–10].

METHODOLOGY FOR DISTINGUISHING MECHANISMS

When we began our studies in this area, methodology for distinguishing between the simple and complex mechanisms shown in Fig. 2 had not yet been developed. It is useful to define steady-state and non-steady-state in reactions following complex mechanisms in terms of the kinetic response as illustrated in Fig. 2. For a reaction at steady state, the decay in reactant concentration is equal to the rise in product concentration at all times, while the decay in reactant concentration leads the rise in product concentration under non-steady-state conditions. These relationships assume that the reactant/product stoichiometry is equal to unity. The relationships in Fig. 2 suggest a number of mechanism probes to distinguish between the simple mechanism and the complex mechanism under non-steady-state conditions (Fig. 3).

Steady-state (at all times):
$-d[R]/dt = d[P]/dt$
Non-steady-state (initial rates):
$-d[R]/dt > d[P]/dt$

$k_{init} > k_{s.s.}$ if reactant is monitored
$k_{init} < k_{s.s.}$ if product is monitored

Fig. 2 Steady-state vs. non-steady-state.

Extent of reaction–time profiles
Rate constant ratio–k_{init}/k_{pfo}
Time ratios–$t_{0.50}/t_{0.05}$
Extent of reaction-dependent deuterium KIE
Wavelength-dependent kinetic response
Instantaneous rate constant–time profiles

Fig. 3 Mechanism probes.

Practical aspects of the mechanism analysis

Before describing the various mechanism probes in more detail, I will present a brief summary of how we carry out our stopped-flow spectrophotometric studies. We prefer to employ low values of the time constant during our measurements using the HiTech SF-61 stopped-flow spectrometers. This results in absorbance–time profiles that have not been subjected to analog smoothing. We typically select a time/point setting that allows recording 2000 data points over slightly longer times than the first half-life. We then smooth the data digitally using the Savitsky–Golay method [13]. The procedure is a sliding 15-point least-squares procedure. The initial operation is applied to the first 15 points and results in the smoothed data point 8. Next, points 2 to 16 are treated in the same way to generate smoothed data point 9. The procedure is continued until all 2000 points have been used, with the overall result of smoothed data points 8–1993.

There is an unavoidable uncertainty in the time-scale when using stopped-flow spectrophotometry due to the dead time of the instrument. The dead times of our two HiTech SF-61's are of the order of 4 ms. We have found that we can very effectively eliminate the uncertainty due to the dead times of the instruments by linear extrapolation of smoothed data points 8–58 to zero time (extent of reaction equal to 0.05 is typically in the range from points 100 to 200). This procedure results in an *effective absorbance* at zero time. The latter is essential to define the extent of the reaction–time scale. The linear extrapolation of theoretical simple mechanism absorbance–time data under the same conditions results in an error of less than 0.03 % in the zero time absorbance.

The ability to differentiate between mechanisms on the basis of best-fit to theoretical extent of reaction–time profiles is often dependent upon the precision in the kinetic measurements. It is sometimes assumed that rate constants obtained by spectrophotometric methods are reliable to about ±5 % [14]. Obviously, precision in a set of measurements can be much greater than the expected reliability of a single measurement. When making multiple repetitions of a measurement, it is appropriate to use the standard error of the mean ($\sigma/N^{0.5}$), where σ is the standard deviation and N is the number of measurement, to express the uncertainty in the mean value [15]. Thus, the best value of the quantity measured (X_{best}) is given by eq. 1, which shows that the uncertainty decreases with the square root of the number of measurements. We have found that $\sigma/N^{0.5}$ of the order of 0.5 % of X_{mean} can be achieved in well-behaved systems by making 60–100 repetitive measurements. In general, we are confident

$$X_{best} = X_{mean} \pm \sigma/N^{0.5} \quad (1)$$

that when our numerical probes values differ from those for the simple mechanism by as much as 5 % that the observed deviations are significant and that the data are inconsistent with the simple mechanism.

Extent of reaction–time profiles

The most common method used to evaluate absorbance–time profiles is to fit the experimental data to an exponential function and evaluate the resulting rate constant. Although this method of data analysis gives excellent results when it is known with certainty that the reaction follows first-order or pseudo-first-order kinetics, it has the very serious drawback that small deviations from first-order kinetics are masked and go unnoticed.

This situation is clearly illustrated by the two different graphical treatments of the same data shown in Fig. 4. The kinetic data are for the Diels–Alder reaction between anthracene (ANTH) and tetracyanoethylene (TCNE) in acetonitrile, which follows the complex mechanism. The figure on the left is the least-squares plot of theoretical ln [Anthracene] vs. time data under pseudo-first-order conditions. Small deviations from linearity are observed at short times, but it is obvious that in the presence of experimental scatter in the data these would be buried in noise and would go undetected. The figure on the right is for the same theoretical data plotted as an extent of the reaction–time profile. The simple mechanism line is normalized to the theoretical data (solid circles) at extent of reaction equal to 0.05. The deviation of the simple mechanism line from the data points is obvious and can only lead to the conclusion that the data are inconsistent with the simple mechanism.

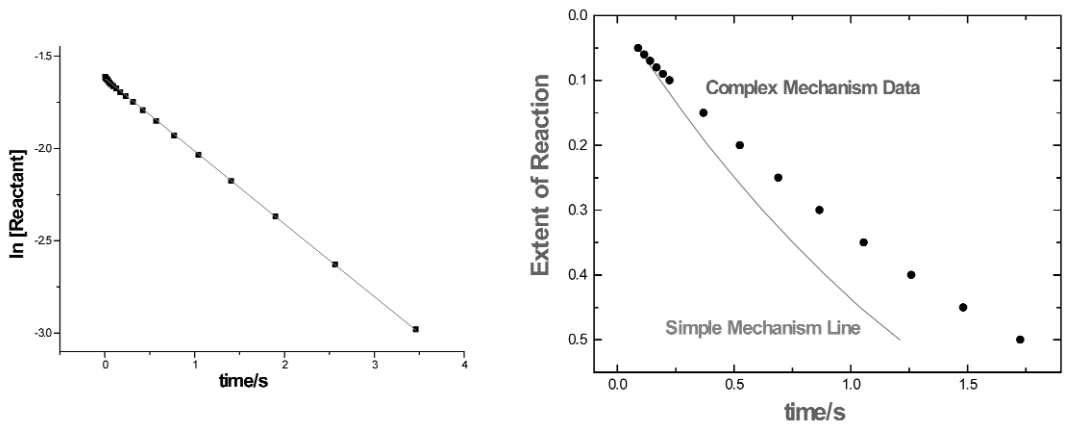

Fig. 4 Graphical representation of kinetic data.

Numerical mechanism probes (k_{init}/k_{pfo} and $t_{0.50}/t_{0.05}$)

The values of the numerical mechanism probes k_{init}/k_{pfo} (the ratio pseudo-first-order rate constants measured in the extent of reaction ranges from 0 to 0.05 and 0.05 to 0.50, respectively) and $t_{0.50}/t_{0.05}$ (the half-life divided by the time necessary to reach the extent of reaction equal to 0.05) are invariant at 1.00 and 13.51, respectively, for a reaction following the simple mechanism, but are dependent upon whether reactant or product is monitored for a reaction following the reversible consecutive second-order mechanism under pseudo-first-order conditions (Fig. 5). In the limit where the two mechanisms are kinetically indistinguishable, the mechanism probe values for the complex mechanism are equal to those for the simple irreversible second-order mechanism (under pseudo-first-order conditions). Obviously, the ability to distinguish between the two mechanisms depends strongly on the precision of the measurements. This aspect of the mechanism analysis was discussed in a previous section.

Irreversible second-order mechanism:
$k_{init}/k_{pfo} = 1.00$
$t_{0.50}/t_{0.05} = 13.5$
Reversible consecutive second-order mechanism:
Monitor reactant: $k_{init}/k_{pfo} \geq 1.00$
$t_{0.50}/t_{0.05} \geq 13.5$
Monitor product: $k_{init}/k_{pfo} \leq 1.00$
$t_{0.50}/t_{0.05} \leq 13.5$

Fig. 5 Mechanism probe values.

Extent of reaction-dependent deuterium kinetic isotope effects

Because of the fact that the intermediate in the complex mechanism partitions between return to reactants and irreversible product formation, the apparent deuterium kinetic isotope effect (KIE_{app}) is attenuated and can be considerably smaller than the real value (KIE_{real}), which is equal to k_p^H/k_p^D, the ratio of the product-forming rate constants for H and D substrate, respectively [1,3]. This has the important consequence that possible hydrogen atom, hydride or proton tunneling may be masked when evaluating KIE_{app}. The mechanism probe is readily applied with a high degree of precision, and its observation gives a clear indication of deviation of experimental data from that expected for the simple mechanism. It also has the advantage that when data from only one of the H or D substrates deviate significantly from simple mechanism behavior, the observation of extent of reaction dependence of KIE_{app} allows for the resolution of the kinetics into the microscopic rate constants for the complex mechanism.

Wavelength-dependent kinetic response

For reactions following the simple mechanism (1 – E.R.) is expected to be independent on whether reactant or product is monitored and on the wavelength at which measurements are made. It is obvious from the mechanism probe values shown in Fig. 5 that this is not the case for reactions following the complex mechanism. We commonly make measurements at 10-nm intervals over the entire applicable range of absorbance. The ideal experimental situation is when measurements can be made at wavelengths where reactant and product are the only absorbing species. In any event, the observation that mechanism probe values are dependent upon the wavelength at which measurements are made is convincing evidence that the kinetics of the reaction are inconsistent with the simple mechanism.

Instantaneous rate constant–time profiles

The value of having access to instantaneous rate constants over the entire time period of the reaction is obvious. These parameters are generally not available, and kinetic data are not generally considered to be of high enough quality to allow the measurement of rate constants over an infinitesimal time period. We have recently found [16] that absorbance–time profiles over a limited range of time can be fit to 5th-order polynomials which reproduce the true values of absorbance to a very high degree of precision. Having extent of reaction–time data in the form of a polynomial equation provides the vehicle for evaluation of instantaneous rate constant–time profiles. The figures in Fig. 6 illustrate the application of this mechanism probe. The extent of reaction–time profiles from which the instantaneous rate constants were derived are theoretical data based upon the microscopic rate constants previously evaluated for the Diels–Alder reaction (10). All of the rate constants in the figures are first-order in units of s^{-1} and k_f' is equal to k_f[TCNE], with the latter in large excess. The figure on the left is for [TCNE] = 160 mM, and that on the right is for [TCNE] = 20 mM. The uppermost curves represent data from decay of reactant (k_{react}), and the lower curves represent data for product formation (k_{prod}). The flat portions of the curves represent steady-state data where the two rate constants are equal (k_{equal}). The figures suggest that a steady state is achieved at extent of reaction equal to about 0.07 at the higher [TCNE] and at about 0.09 at the lower [TCNE]. Another feature of interest is that the k_{react} curve intersects 0 extent of reaction at a value equal to k_f'. The intercept value for k_{prod} is zero and is of less practical interest. The intercept for the k_{react} plot suggests the possibility of evaluating the forward rate constant (k_f) directly from experimental data without the necessity of the complete resolution of the kinetics.

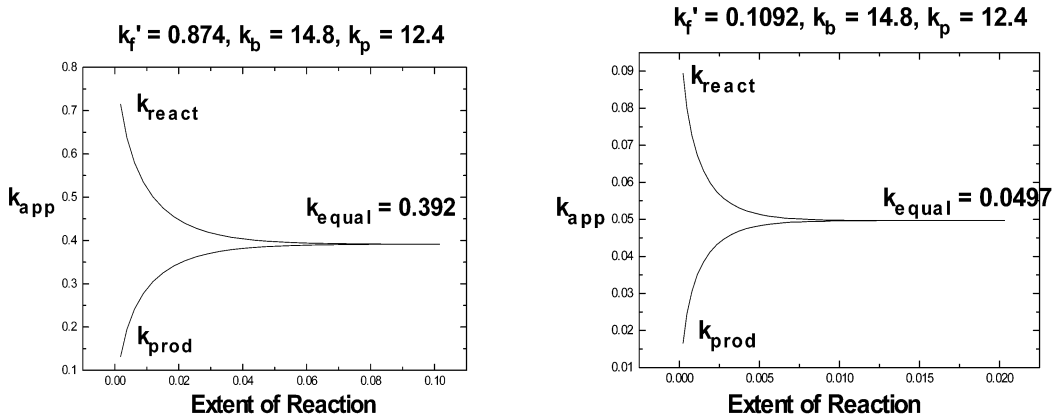

Fig. 6 Instantaneous rate constant: extent of reaction profiles.

The developments described in the previous paragraph are very recent [16], and we have not yet applied this mechanism probe to experimental data. I anticipate that instantaneous rate constant–time profiles potentially represent the ultimate chemical kinetics mechanism probe. Obviously, application of this mechanism probe to kinetic data for the simple mechanism or that for the complex mechanism at the limit where the mechanisms are kinetically indistinguishable results in a single straight line with zero slope independent of whether reactant or product is monitored.

Non-steady-state kinetic studies

The collective application of the mechanism probes can be referred to as non-steady-state kinetic studies. The procedure involved is illustrated in Fig. 7. The initial experiments are directed toward the application of the mechanism probes in order to determine whether the kinetic data deviate significantly

from that for the simple mechanism. If significant deviations are observed, this suggests a complex mechanism and the possibility of resolving the kinetics into the microscopic rate constants for that mechanism. The latter can be achieved using a detailed data-fitting procedure involving the concurrent analysis of extent of reaction–time profiles at three different second reactant concentrations or alternatively with extent of reaction–time profiles for both H and D substrate for proton- or hydride-transfer reactions.

Mechanism analysis:

Compare experimental extent of reaction–time profiles in the *pre-steady-state time period* with theoretical profiles for the simple irreversible second-order mechanism

Resolution of the kinetics:

Detailed comparison of experimental data to theoretical data in order to evaluate the best-fit microscopic rate constants for the complex mechanism.

Fig. 7 Non-steady-state kinetic studies.

It is highly likely that the instantaneous rate constant–time profiles discussed in the previous section can be developed to entail both the mechanism analysis and kinetic resolution features of the non-steady-state kinetic method.

Dynamic residual absorbance analysis

A lofty objective of any mechanism study is to characterize any intermediates that may lie on the reaction coordinate. This is always a very difficult and sometimes impossible task. The intermediates are, by definition, short-lived and are usually present in very low concentrations. Furthermore, the absorbance due to intermediates is most often buried in the much larger absorbances of reactants and products present in higher concentrations. It occurred to us that it should be possible to extract the absorbance due to an intermediate if we make use of all of the kinetic data at our disposal. It is usually possible to find a wavelength where only reactant or product have significant absorbance. Under these conditions, the kinetics of the complex mechanism can be resolved, giving access to the microscopic rate constants which in turn can be used to calculate absorbance–time profiles of both reactant and product. The procedure that we have developed over the past two years is illustrated in Fig. 8. The procedure is best illustrated with an example. At the present time, we are applying the method using only single wavelength measurements, but further development to diode-array spectral data is expected to involve a straight-forward extension of the present procedure. The absorbance–time profiles shown in Fig. 9 refer to the S_N2 reaction between *p*-nitrophenoxide ion and methyl iodide in acetonitrile. At 450 nm, *p*-nitrophenoxide ion is the only absorbing species present. The uppermost absorbance–time profile (total) was recorded at 330 nm after resolution of the kinetics at 450 nm. The absorbance–time profiles of reactant and product were then calculated and are shown in the figure on the left. After subtracting out the absorbance–time profiles for reactant and product, the uppermost absorbance–time profile in the figure on the right is that obtained by a trial-and-error search for the best value of the intermediate extinction coefficient to give the lowest average value of the residual absorbance. The latter was observed to be less than 10^{-3} absorbance units in this case. The average residual absorbance is not expected to equal zero since all of the experimental error will show up in this quantity. The trial-and-error procedure for converting the calculated [Intermediate]–time profile to the corresponding absorbance–time profile generally requires from 5000 to 10 000 iterations. The figures in Scheme 3 refer to data at a single wavelength, 330 nm. To obtain a spectrum of the intermediate, it is necessary to repeat this procedure at every accessible wavelength.

Procedure:

(a) Resolve the kinetics at λ where only R or P absorb (to evaluate k_f, k_b, k_p).
(b) Subtract calculated absorbance due to reactants and product from the total absorbance (this gives residual absorbance–time profiles at all λ).
(c) Fit the residual absorbance–time profiles to the calculated [I] – t profile to determine the intermediate extinction coefficient at all λ.
(d) Plot intermediate absorbance vs. λ to obtain the spectrum.

Fig. 8 Dynamic residual absorbance analysis (DRAA).

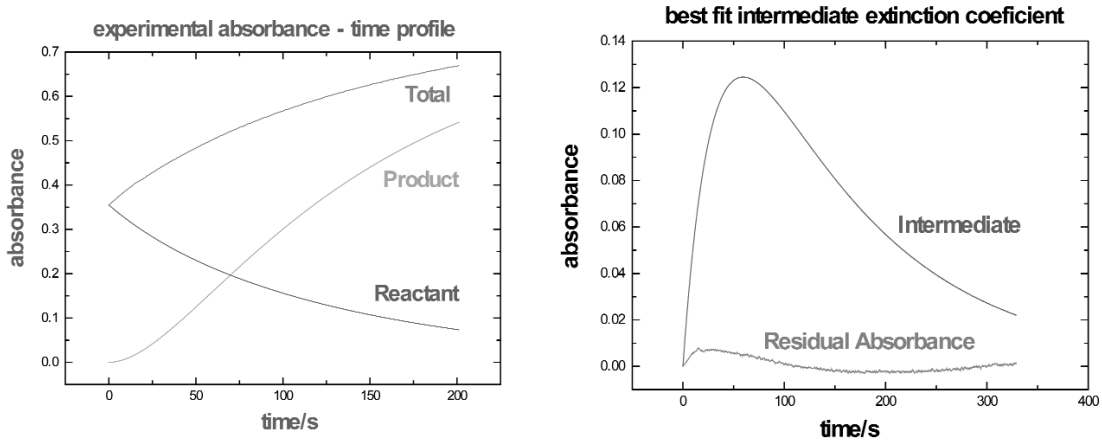

Fig. 9 Graphical description of the dynamic residual absorbance analysis.

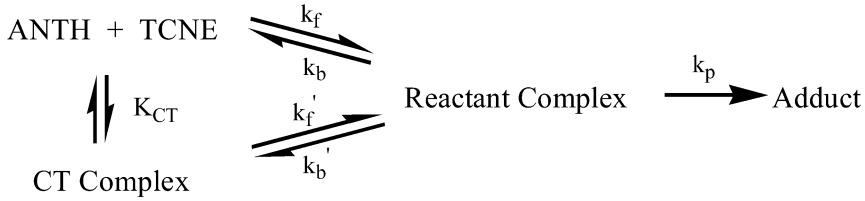

Scheme 3

NON-STEADY-STATE KINETIC STUDIES

An example of a non-steady-state kinetic study

For the sake of brevity, I will restrict the discussion of the application of the non-steady-state kinetic method to a single example. More detailed descriptions can be found in refs. [1–10].

The reaction between ANTH and TCNE represents an example of a number of Diels–Alder reactions during which charge-transfer (CT) complexes are known to form [10]. Whether or not the CT complex lies on the reaction coordinate for adduct formation has been discussed in detail over the years [17–22]. Kiselev and Miller [21] offered the observation of a negative Arrhenius activation energy during the reaction between 9,10-dimethylanthracene and TCNE as proof that the CT complex indeed does lie on the reaction coordinate for adduct formation. Wise and Wheeler [22] concluded that their theoretical results unambiguously establish that the CT complex lies on the lowest energy pathway for adduct formation during the reaction of ANTH with TCNE in chloroform.

Our mechanism probe data [10] for the reaction between ANTH and TCNE in acetonitrile at 293 K are summarized in Table 1. The experimental data $t_{0.50}/t_{0.05}$ and k_{init}/k_{pfo} are in columns labeled

"Observed" and theoretical data are in columns labeled "Theory". The latter were derived using the best-fit rate constants shown in footnote b. At the lowest $[TCNE]_o$ (20 mM), the values of the mechanism probes deviate only slightly from the expected values for the simple mechanism equal to 13.5 ($t_{0.50}/t_{0.05}$) and 1.00 (k_{init}/k_{pfo}), respectively. However, as $[TCNE]_o$ was increased, the deviations from simple mechanism behavior became substantial. The assumption of equal extinction coefficients of ANTH and the Reactant Complex (Scheme 3) was necessary for the data obtained at 320 nm, and the close correspondence between the experimental and theoretical values of the mechanism probes was not necessarily expected.

Table 1 Experimental and theoretical time and rate constant ratios for the reactions of ANTH with TCNE at 293.2 K[a].

		$(t_{0.50}/t_{0.05})$		(k_{init}/k_{pfo})	
$[TCNE]_o$ mM	λ/nm	Observed	Theory[b]	Observed	Theory[b]
20	380	13.7	14.1	1.02	1.05
40	380	14.7	14.7	1.09	1.09
80	380	16.1	16.1	1.21	1.21
160	380	19.6	19.3	1.50	1.46
20	320	13.2	13.2	0.98	0.97
40	320	12.9	12.9	0.95	0.93
80	320	12.4	12.3	0.91	0.88
160	320	11.1	10.8	0.81	0.78

[a]At 320 nm, the assumption that the extinction coefficient is the same for the intermediate as for ANTH was necessary; extent of reaction = $1 - ([ANTH] + [Intermediate])/[ANTH]_o = [Adduct]/[ANTH]_o$.
[b]Theoretical data for the reversible consecutive second-order mechanism with $k_f = 5.46\ M^{-1}\ s^{-1}$, $k_b = 14.8\ s^{-1}$, and $k_p = 12.4\ s^{-1}$.

The CT complex between ANTH and TCNE (λ_{max} = 657 nm) was observed to form during the time of mixing in stopped-flow studies and was ruled out as the intermediate, giving rise to the deviations from simple second-order kinetics. As shown in Scheme 3, our kinetic data are inclusive regarding the participation of the CT complex on the reaction coordinate leading to adduct formation. However, we suggested that the reactant complex is most likely formed by extrusion of solvent from the CT complex.

Comments on the structures of intermediates in the complex mechanism

All of the reactions on which we have applied the non-steady-state kinetics methodology [1–10] are relatively slow, with half-lives ranging from several hundred milliseconds to about 100 seconds. Yet, we have proposed that the intermediate (reactant complex) forming reactions, that necessarily take place on the same time scale as the overall reaction, do not involve the creation of new covalent bonds. This may appear to represent an inconsistency since nonbonded complexes such as the encounter complexes, ion-pairs, and CT complexes are formed at or near diffusion-controlled rates.

Let us consider, as an example, our proposal for the nature of the "reactant complex" in the Diels–Alder reaction discussed in the previous section. As mentioned, we do not have any kinetic evidence suggesting that the CT complex is on the reaction coordinate leading to product formation in acetonitrile solvent. However, theoretical calculations [22] suggest that the CT complex lies on the product-forming reaction coordinate for the reaction carried out in chloroform. The barrier for CT complex formation appears to be very small, and density function calculations [23] suggest that the reactant

moieties lie in parallel planes with an interplanar distance of 3.40 Å. Since the carbon atoms involved in bond formation have the proper orientation in the CT complex, it appears reasonable to assume the latter is indeed on the product-forming reaction coordinate. Our proposal is that this is the case and that the conversion of the CT complex to the "reactant complex" is accompanied by the shortening of the distances between the reaction centers and the extrusion of solvent, giving rise to a significant reaction barrier, as illustrated in Scheme 4. In Scheme 4, the interactions shown on the left are the lowest unoccupied molecular orbital (LUMO) of TCNE and the highest occupied molecular orbital (HOMO) of ANTH.

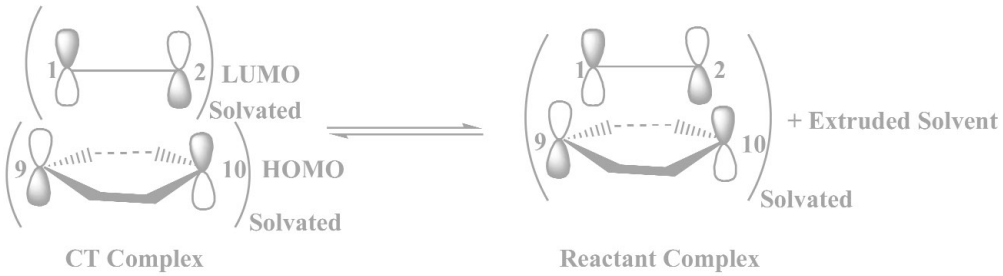

Scheme 4

Similar considerations can be employed to suggest the formation of the "reactant complex" in other reactions that involve significant reaction barriers. For example, we suggest ion–dipole complexes as the pertinent intermediates in nitroalkane proton-transfer reactions in aqueous solutions, in the S_N2 reaction between *p*-nitrophenoxide ion and methyl iodide in acetonitrile [7,9] and in the elimination reactions of *p*-nitrophenethylhalides [6] in protic solvents. The example chosen to illustrate ion–dipole complex formation (Scheme 5) is for the proton-transfer reaction between an aryl nitroalkane and hydroxide ion [2] in aqueous acetonitrile.

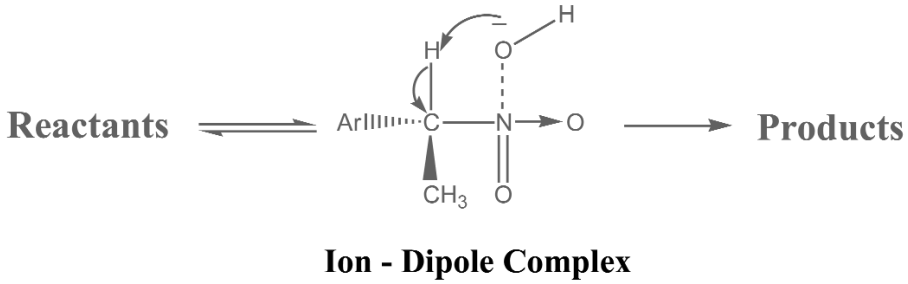

Scheme 5

CONCLUSIONS

The question, "Is the single transition-state model appropriate for the fundamental reactions of organic chemistry?", has not yet been definitely answered. Our work over the past five years serves to sow the seeds of doubt on the general applicability of this concept, which has dominated the thinking of physical organic chemists for more than half a century. We have observed that several different classes of organic reactions that have previously been treated as simple second-order processes fail to pass the tests provided by our mechanism probes. On the other hand, the kinetics of all of these reactions are readily accommodated by the reversible consecutive second-order mechanism and we have succeeded in the resolution of the kinetics to the microscopic rate constants of that mechanism. Our studies in this area have slowed down due to the necessity of developing the procedures capable of differentiating be-

tween the simple and complex mechanisms. It is my opinion that our efforts up to now have served to uncover the tip of the iceberg and that further probing of this area in the future may possibly bring about a profound change in the thinking of physical organic chemists and the way they approach the study of organic reaction mechanisms.

REFERENCES

1. V. D. Parker, Y. Zhao, Y. Lu, G. Zheng. *J. Am. Chem. Soc.* **120**, 12730 (1998).
2. Y. Zhao, Y. Lu, V. D. Parker. *J. Am. Chem. Soc.* **123**, 1579 (2001).
3. V. D. Parker and Y. Zhao. *J. Phys. Org. Chem.* **14**, 604 (2001).
4. Y. Lu, Y. Zhao, V. D. Parker. *J. Am. Chem. Soc.* **123**, 5900 (2001).
5. Y. Zhao, Y. Lu, V. D. Parker. *J. Chem. Soc., Perkin Trans. 2* 1481 (2001).
6. K. L. Handoo, Y. Lu, Y. Zhao, V. D. Parker. *Org. Biomol. Chem.* **1**, 24 (2003).
7. Y. Lu, K. L. Handoo, V. D. Parker. *Org. Biomol. Chem.* **1**, 36 (2003).
8. Y. Lu, Y. Zhao, K. L. Handoo, V. D. Parker. *Org. Biomol. Chem.* **1**, 173 (2003).
9. V. D. Parker and Y. Lu. *Org. Biomol. Chem.* **1**, 2621 (2003).
10. K. L. Handoo, Y. Lu, V. D. Parker. *J. Am. Chem. Soc.* **125**, 9381 (2003).
11. M. Eigen and J. S. Johnson. *Annu. Rev. Phys. Chem.* **11**, 309 (1960).
12. L. P. Hammett. *Physical Organic Chemistry*, 2nd ed., McGraw Hill, New York (1940); Tokyo (1970).
13. A. Savitsky and M. Golay. *Anal. Chem.* **36**, 1627 (1964).
14. J. F. Bunnett. In *Investigation of Rates and Mechanisms of Reactions, Part 1: General Considerations and Reactions at Conventional Rates*, 3rd ed., E. S. Lewis (Ed.), Chap. 4, John Wiley, New York (1974).
15. J. T. Taylor. *An Introduction to Error Analysis*, University Science Books, Oxford University Press, Mill Valley, CA (1982).
16. V. D. Parker. Work in progress.
17. P. Brown and R. C. Cookson. *Tetrahedron* **21**, 1977 (1965).
18. N. D. Epiotis. *J. Am. Chem. Soc.* **94**, 1924 (1972).
19. C. C. Thompson and D. D. Holder. *J. Chem. Soc., Perkin Trans. 2* 257 (1972).
20. L. J. Andrews and R. M. Keefer. *J. Am. Chem. Soc.* **77**, 6248 (1955).
21. V. D. Kiselev and L. G. Miller. *J. Am. Chem. Soc.* **97**, 4036 (1975).
22. K. E. Wise and R. A. Wheeler. *J. Phys. Chem. A* **103**, 8279 (1999).
23. M. S. Liao, Y. Lu, S. Scheiner. *J. Comput. Chem.* **24**, 623 (2003).